RSC Advances

PAPER

View Article Online
View Journal | View Issue

Cite this: *RSC Adv.*, 2018, **8**, 39787

Effect of different factors on the yield of epoxy-terminated polydimethylsiloxane and evaluation of CO_2 thickening

Yanling Wang,†[a] Qiang Li,†*[a] Weihong Dong,[c] Qingchao Li,[a] Fuling Wang,[b] Hao Bai,[a] Ren Zhang[a] and Augustus Boadi Owusu[a]

Received 31st July 2018
Accepted 13th November 2018

DOI: 10.1039/c8ra06430j

rsc.li/rsc-advances

We focused on optimizing synthetic parameters based on a Taguchi design to maximize polymer yield and evaluate the polymer-thickening ability in CO_2. The stirring speed, reaction temperature, catalyst content, and reaction time were the major control parameters (independent variables) in these two individual reactions. The signal-to-noise ratio (S/N ratio) obtained under each experimental condition was utilized to evaluate the optimum preparation process for the maximum yield. A maximum yield of 87.20% in a ring-opening polymerization was reported, and the optimum conditions were 70 °C, 2.0 g of sulfuric acid, and stirring speed of 110 rpm. Temperature, however, was the most effective factor. Similarly, research of hydrosilylation obtained a maximum yield of 84.7% under optimum conditions of 100 °C, chloroplatinic acid of 0.003 wt%, and stirring speed of 190 rpm. Also, we measured CO_2 viscosity based on different concentrations of thickener at different temperatures, pressures and flow rates. Epoxy-terminated polydimethylsiloxane could be used for CO_2 fracturing to obtain excellent fracturing.

1. Introduction

As an important method to enhance crude-oil production, several shortcomings have hindered the application of hydraulic fracturing.[1] By contrast, CO_2 fracturing technology can be used to form fractures in reservoirs based on advantages such as a fewer environmental hazards and greater fracturing efficiency.[2–4] However, the lower proppant-carrying property, caused by low CO_2 viscosity, is considered the biggest challenge to application of CO_2 in fracturing technology.[1,5] To improve CO_2 viscosity, a thickener with an excellent thickening property should be added to liquid CO_2.

Fluoropolymers and hydrocarbon polymers[6,7] are considered excellent thickeners to improve the CO_2 viscosity. However, many defects have been revealed during CO_2 fracturing.[8] As a result, several scholars have reported that silicone can thicken liquid CO_2.[5,9,10] Nonetheless, it remains a principal challenge to increase the poor solubility and thickening capability in liquid CO_2.[11] To increase the thickening property of silicone in liquid CO_2, researchers have employed chemical modification, polymer grafting and co-solvent assistance.[11] Excessive addition of a co-solvent resulted in excellent solubility in CO_2, but was deemed unwise and expensive. By contrast, chemical modification and polymer grafting is conducive to designing a silicone thickener with excellent solubility and thickening capability in liquid CO_2.

In chemical modification, optimizing the preparation condition did not increase the product yield only, but also reduced the cost of CO_2 fracturing significantly. For most chemical reactions, the stirring speed, temperature, time and catalyst content have a huge influence on the yield over the preparation process. In general, many experiments based on the factors stated above were conducted to discover the optimal preparation condition with a maximum yield. Meanwhile, more experiments were carried out involving increasing the number of independent variables. It was not only a tedious task to screen for an optimal process with maximum yield, but also a huge cost in each experiment. As an excellent optimized method, the experimental design of Taguchi and colleagues was utilized to obtain the optimal combination with a small number of experiments.[12,13] Also, interactions between two variables could be modelled using orthogonal arrays (OAs).[14] Moreover, the reduced sensitivity of the system to variation sources was shown in this optimized method.[15]

We wished to design and synthesize a modified epoxy-terminated polydimethylsiloxane, optimize the preparation condition of a polymer by the Taguchi design, and investigate the influence of selected parameters on the yield. In addition, the thickening property of epoxy-terminated polydimethylsiloxane in CO_2 was measured and evaluated.

[a]College of Petroleum Engineering, China University of Petroleum (East China), Qingdao, 266580, China. E-mail: B16020083@s.upc.edu.cn

[b]School of Science, China University of Petroleum (East China), China

[c]Branch Company of Exploration and Production, CNPC, Beijing 100011, China

† Yanling Wang and Qiang Li contributed to the work equally and should be regarded as co-first authors.

2. Experimental

2.1 Materials

All cyclosiloxanes and chain siloxanes were procured from Jiande City Sifco Materials (China). Ethanol, toluene and chloroplatinic acid were obtained from Nanjing Chemical Reagents (China). Moreover, sulfuric acid was purchased from Sinopharm Chemical Reagents (China). Tetramethyldisiloxane and glycidyl methacrylate were sampled as received without further purification. However, the polyacrylate polymer water-absorbing resin was added into ethanol (95%) with a mass ratio of 1 : 4 for 150 min. A sieve (120 mesh) was used to separate the water-absorbing resin and obtain purified ethanol. For toluene purification, it was first passed through two adsorption columns packed with alumina and diatomaceous each, respectively, at 50 mL min^{-1}. Toluene was then dried with a desiccant (potassium carbonate) at 60 mL min^{-1}. The dried toluene was injected into a rectification tank at 120 °C to obtain toluene at 99.5% purity. To remove hexamethylcyclotrisiloxane in octamethylcyclotetrasiloxane, a distillation tower with 50 theoretical plates was employed at 0.03 MPa, and a distillation tower with 60 theoretical plates was used to obtain octamethylcyclotetrasiloxane at 99.9% purity.

2.2 Preparation of epoxy-terminated polydimethylsiloxane

First, 60 g of octamethylcyclotetrasiloxane (D4) and 0.1 g of sulfuric acid were poured into a flask, and then 5 g of tetramethyldisiloxane was dripped into this flask for 10 min. The solution was stirred at constant temperature for >5 h. To obtain the pure primary product, 2 g of sodium carbonate was added to neutralize sulfuric acid, and filtering was conducted to clean up the sodium sulfate generated. Water was separated by stratification between the primary product and water, and the clear primary product was dried in a vacuum drying oven at 70 °C and at vacuum pressure of 0.9 kPa. After cooling to room temperature, the primary product was transferred to another flask, hydrosilylation was conducted by the addition of glycidyl methacrylate (GM) and chloroplatinic acid, and stirring was continued for >3 h. After completion of hydrosilylation, 2 g of activated carbon was added to remove chloroplatinic acid, and vacuum distillation employed to separate the remaining glycidyl methacrylate at 105 °C and at a vacuum pressure of 1.1 kPa. Molecular weight (M_n = 21 000) of the final product was determined using an Ubbelohde viscometer, and 89.2% of silicone repeat units were obtained by titration (Fig. 1).

As shown in Fig. 2, the peak at 2963 cm^{-1} was viewed as the C–H stretching vibrations of CH_3, stretching vibrations of Si–H were expressed at 2121 cm^{-1}, and the sharp peak at 1416 cm^{-1} indicated the asymmetric vibration of Si–CH_3. By contrast, the symmetrical vibration of CH_3 was presented at 1264 cm^{-1}, and the peaks observed at 1090 and 1021 cm^{-1} were attributed to the symmetrical stretching vibration of Si–O–Si.[1] In addition, the telescopic vibration of Si–C was viewed at 800 cm^{-1}.

Epoxy-terminated polydimethylsiloxane (orange) presented prominent peaks at 2972, 1740, 1170, 1018, 1090, 1021 and 800 cm^{-1}. The bending vibration at 1740 cm^{-1} showed the

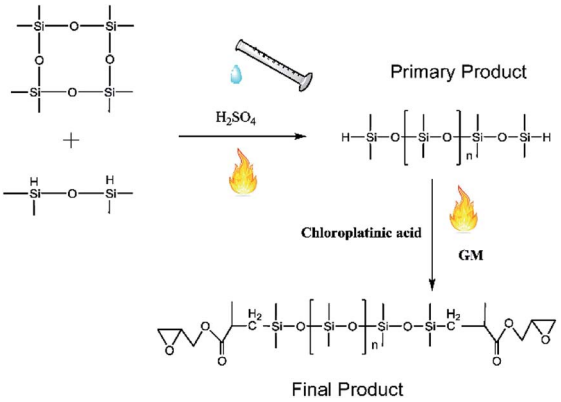

Fig. 1 Preparation of epoxy-terminated polydimethylsiloxane.

C=O bond on it. The strong adsorption bands at 1170 and 1018 cm^{-1} were the characteristic stretching vibrations of the C–O–C group and epoxy group, respectively.[16] Meanwhile, the peak between 850 and 912 cm^{-1} was viewed as the epoxy-ring vibration band.[16]

^{1}H-NMR ($CDCl_3$): δ 0.11 (m, 924H), 0.69 (m, 4H), 1.19 (m, 6H), 1.89 (s, 2H), 3.86 (m, 2H), 4.34 (d, 2H), 3.17 (s, 2H), 2.54 (s, 2H), 2.79 (s, 2H), 7.39 (s, $CDCl_3$).

The epoxy-terminated polydimethylsiloxane was characterized by the weak peaks of the epoxy group at 2.54 (h), 2.79 (i) and 3.17 ppm (g)[17] (Fig. 3). Furthermore, the H (a) of the methyl group connected to a Si appeared at 0.11 ppm (δ). The peak at 0.69 ppm was ascribed to the methylene H (b). The chemical shift of Si–H at 4.5–5.0 ppm and that of H in the C=C bond at 5.0–5.8 ppm were discovered separately. These chemical shifts showed a complete ring-opening polymerization and hydrosilylation. All these results demonstrated that the epoxy group was introduced quantitatively to the final product as designed.

2.3 Taguchi design

To find the optimal combination with a maximum yield, many experiments should be carried out. It was necessary to find an effective optimization method which could evaluate interactive

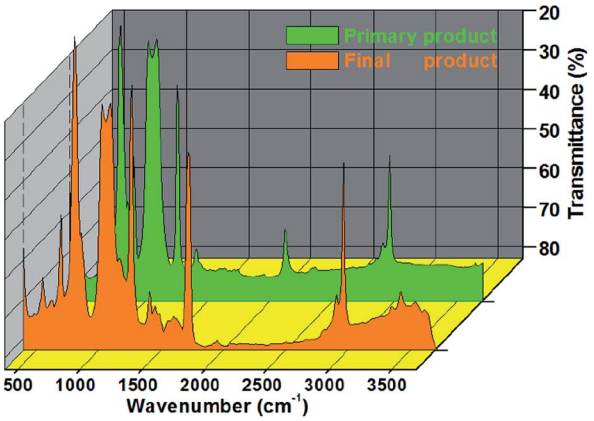

Fig. 2 FTIR spectrum of the product from these two reactions.

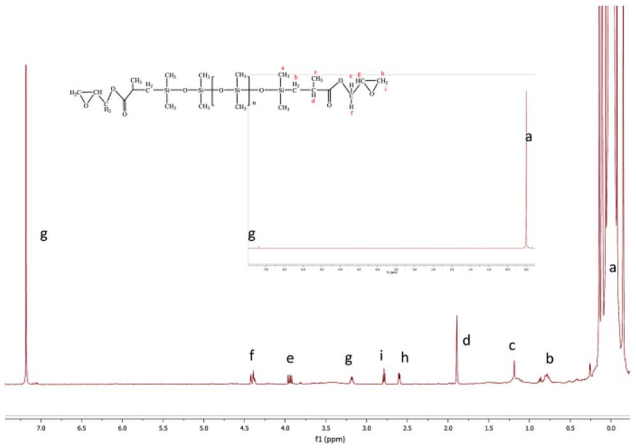

Fig. 3 ^{1}H-NMR ($CDCl_3$) of the final product.

factors to obtain the optimal prepared condition with the maximum yield. The yield was expressed as:

$$y(\%) = \frac{\text{Sample quality after purification (g)}}{\text{Sample quality (g)}} \times 100\% \quad (1)$$

where y was the yield (%).

The Taguchi experimental design is used to optimize parameters and investigate their influence on the yield.[18,19] The evaluated target (yield) was first used to assess the suitability of each combination. Based on the yield, the factors with a significant influence on the yield were screened and the parameter range determined. Then, the orthogonal array design was used to obtain a specific combination, and a yield would be formed in each combination.[20] Then, a signal-to-noise (S/N) ratio (eqn (2)),[21] converted from each observed yield at the orthogonal array design, was employed to evaluate the effect of each factor on the yield so as to determine the optimal combination with a maximum yield.

$$\text{S/N} = -10 \log \frac{1}{n}\left(\frac{1}{y^2}\right) \quad (2)$$

where y is the observed yield and n is the number of experiments.

2.4 Viscosity-measuring device

A modified capillary viscometer (Fig. 4), designed based on the Hagen–Poiseuille law, was divided into a pressurized system, dissolution system and viscosity-measurement system. To remove water in CO_2, a desiccator was installed behind the CO_2 cylinder, and a compression pump used to pressurize CO_2 into a pressure-resistant container. The pressurized CO_2 in the container was injected into the dissolution equipment after the thickener and toluene had been added into the container. The pressure was adjusted slightly by an ISCO pump and a water bath was used to control the temperature of the dissolving device. A window embedded in the dissolving device was utilized to observe the solubility and phase behaviour of the thickened liquid CO_2 at different temperatures and pressures.

After mixing for 30 min, layering was seen. By contrast, a uniformly transparent liquid CO_2 was injected into the container and a viscosity measurement conducted. The liquid CO_2 in the capillary possessed a certain flow (Q), temperature and pressure. The pressure sensor at both ends of the capillary could record differential pressure (ΔP), and each ΔP was converted to fluid viscosity.[22] In the present study, the capillary radius was 0.002 m, and capillary length was 5 m.

2.5 Mechanism of viscosity measurement

For this capillary viscometer, the relationship between the viscosity and ΔP is represented by the Hagen–Poiseuille law, but the latter is suitable for a laminar fluid.[22]

As seen in Fig. 5, a cylindrical fluid with a radius r was considered as an object to explore the mechanism of viscosity measurement. The force F formed by the pressure difference (ΔP) is shown in eqn (3):

$$F = (P_1 - P_2)\pi r^2 \quad (3)$$

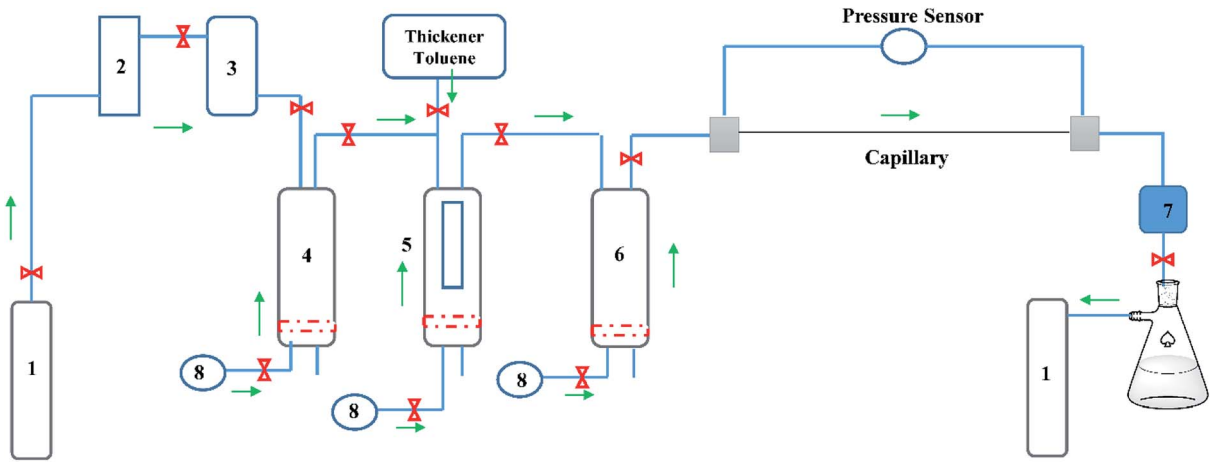

Fig. 4 Capillary viscometers (schematic). (1) CO_2 cylinder. (2) Desiccator. (3) Compression pump. (4) Pressure-resistant gas cylinder. (5) Dissolution-measuring device. (6) Fracturing fluid-storage device. (7) Pressure-control device. (8) ISCO pump.

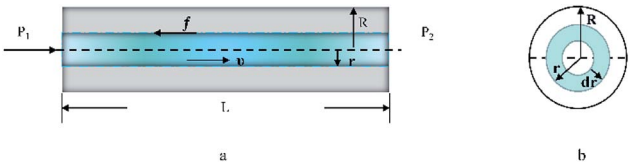

Fig. 5 (a) Flow for a laminar fluid in the capillary (along the direction of the capillary) (schematic). (b) Sectional flow for a laminar fluid in the capillary (along the flow direction of the fluid).

where F is the advancing force, N; P_1 and P_2 present the pressure difference (ΔP) at the ends of the capillary in MPa. Eqn (4) shows the viscous force exerted by other fluids on this cylindrical fluid, and an opposite direction is displayed between F and f.

$$f = \eta 2\pi r L \frac{\mathrm{d}v}{\mathrm{d}r} \tag{4}$$

where f is the resistance in N, η is the fluid viscosity in mPa s, v is the flow rate in m s^{-1}, and L is the capillary length in m. An equal state was shown between eqn (3) and (4) due to the steady flow of this fluid, and then the comprehensive equation is presented by eqn (5).

$$(P_1 - P_2)\pi r^2 = \eta 2\pi r L \frac{\mathrm{d}v}{\mathrm{d}r} \tag{5}$$

Eqn (6) shows an integral equation of eqn (5).

$$v = \frac{(P_1 - P_2)}{4\eta L}\left(R^2 - r^2\right) \tag{6}$$

$$\mathrm{d}Q = v\mathrm{d}S = \frac{(P_1 - P_2)}{4\eta L}\left(R^2 - r^2\right) \times \pi r \mathrm{d}r \tag{7}$$

$$Q = \int_0^R \frac{(P_1 - P_2)}{2\eta L}\left(R^2 - r^2\right) \times \pi r \mathrm{d}r \tag{8}$$

$$Q = \frac{\pi R^4}{8\eta L}(P_1 - P_2) \tag{9}$$

where Q is the flow rate in mL min^{-1}. As shown in Fig. 5b, the liquid flow ring with a radius of r and width of dr is shown in eqn (9) at the premise of laminar flow. The basic equation of apparent viscosity could be obtained by a variant of eqn (9).

The thickening performance of epoxy-terminated polydimethylsiloxane in liquid CO_2 was measured at different conditions. Moreover, because the calculation of the viscosity does not involve the shear rate, the flow rate (Q) was used to calculate the viscosity, thus the shear rate was not discussed.

3. Results and discussion

3.1 Single-factor investigation for ring-opening polymerization

As an important method to optimize preparation conditions, single-factor investigation also provided a range for each factor. Temperature, amount of sulfuric acid, reaction time and stirring speed were considered to be the most important factors in the ring-opening polymerization.

Fig. 6a shows a rising yield with increasing temperature from 30 °C to 70 °C. A stable maximum yield was displayed at each temperature between 30 °C and 70 °C due to an adequate reaction time and catalyst at each temperature. Meanwhile, an increasing yield was observed with increasing temperature from 30 °C to 70 °C, and a gradually decreasing growth rate of yield was shown with an increase in temperature. As seen in the yield at 70 °C, the ring-opening polymerization occurred mainly between 2 h and 4 h, and a high yield was displayed. However, a low yield and long-time range was illustrated at 30 °C. The Taguchi experimental design could be used from 30 °C to 70 °C.

As shown in Fig. 6b, there was no maximum yield when the amount of sulfuric acid was <2 g because sulfuric acid could not cause a sufficient reaction with the other raw materials. By contrast, there was a maximum yield when sulfuric acid was >2 g and was attributed to sufficient catalysis between sulfuric acid and raw materials. However, the yield showed no disparity for each stirring speed shown in Fig. 6c.

3.2 Single-factor investigation for hydrosilylation

A similar trend was shown in the single-factor investigation of hydrosilylation. However, there were obviously different value

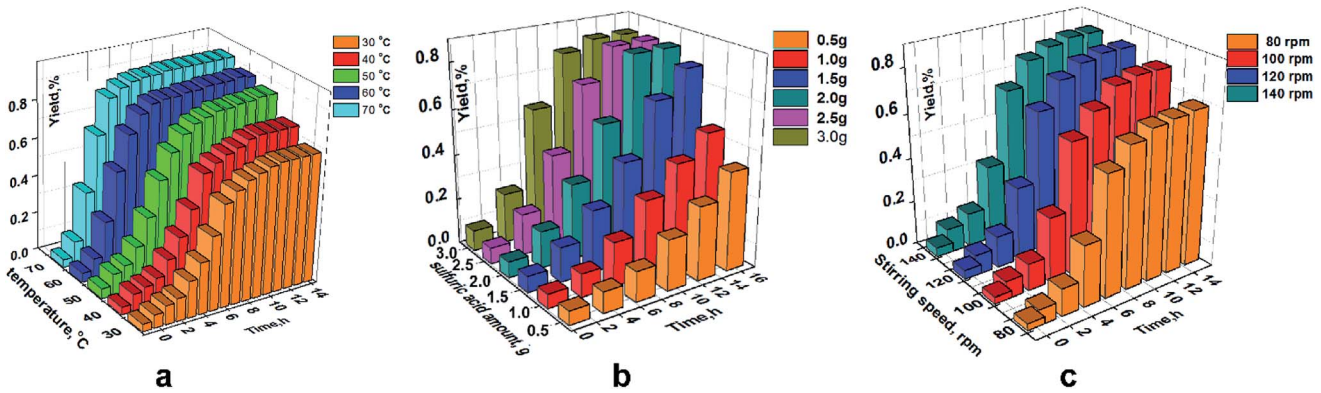

Fig. 6 The effect factors have individually on the yield (ring-opening polymerization). (a) Amount of sulfuric acid is 2.0 g and a stirring speed is 120 rpm. (b) At a temperature of 70 °C and a stirring speed of 120 rpm. (c) At a temperature of 70 °C and sulfuric acid of 2.0 g.

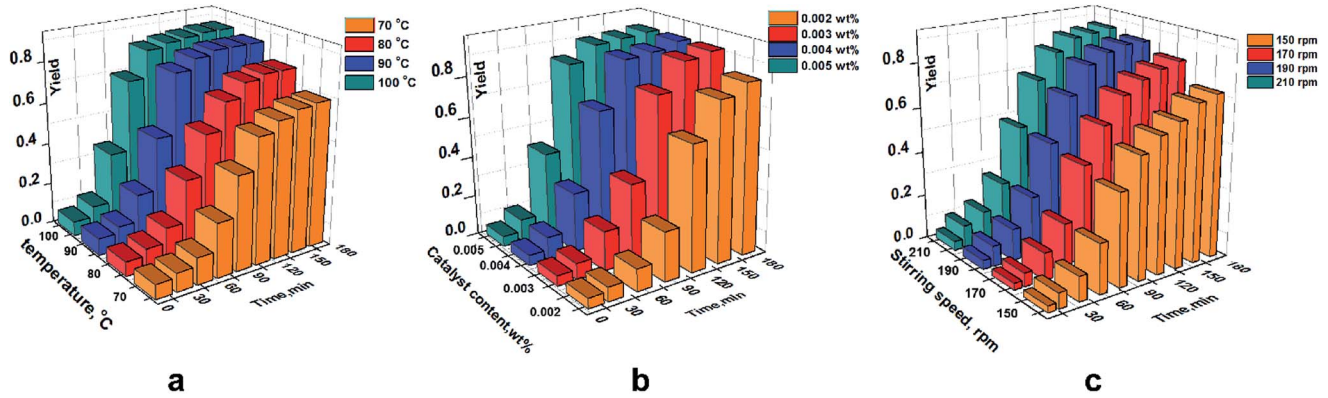

Fig. 7 Effect of individual factors on the yield (hydrosilylation). (a) At chloroplatinic acid of 0.004 wt% and stirring speed of 190 rpm. (b) At 90 °C and stirring speed of 190 rpm. (c) at 90 °C and chloroplatinic acid of 0.004 wt%.

Table 1 Parameters and levels for ring-opening polymerization

Influencing factor	Level 1	Level 2	Level 3	Level 4
A: temperature (°C)	60	70	80	90
B: sulfuric acid amount (g)	0.5	1.0	1.5	2.0
C: stirring speed (rpm)	70	90	110	130

ranges for these influencing factors between ring-opening polymerization and hydrosilylation. Detailed values of these factors and the effect on the yield are illustrated in Fig. 7.

As shown in Fig. 7a, the maximum yield increased gradually when the temperature increased. However, there was no change in the maximum yield after 90 °C. To note the effect of chloroplatinic acid on the yield, a similar trend was revealed. The yield at chloroplatinic acid of 0.004 wt% was almost equal to the maximum yield at 0.005 wt%. Moreover, the yield at 150 rpm was significantly lower than the yield at other speeds (≥170 rpm) (Fig. 7c).

3.3 Optimization of ring-opening polymerization

Table 1 shows that three factors in four levels were chosen to evaluate the best combination with the maximum yield of the ring-opening polymerization. Analysis of variance (ANOVA) was used to study the effect of these factors on the yield and the best combination (Table 2).

A plan with 16 experiments, designed based on the orthogonal array, was carried out in a random sequence.[23] Table 3 shows the detailed experimental design and results. A discerning analysis and analysis of variance (Table 5) were undertaken to obtain the optimized prepared process with the highest yield.

Table 3 Experimental design of ring-opening polymerization

Strain	A, °C	B, g	C, rpm	Yield, %	S/N
1	40	0.5	70	27	28.63
2	40	1.0	90	33	30.37
3	40	1.5	110	42	32.46
4	40	2.0	130	49	33.80
5	50	0.5	90	37	31.36
6	50	1.0	70	43	32.67
7	50	1.5	130	55	34.81
8	50	2.0	110	66	36.39
9	60	0.5	110	49	33.80
10	60	1.0	130	53	34.49
11	60	1.5	70	62	35.85
12	60	2.0	90	72	37.16
13	70	0.5	130	50	33.98
14	70	1.0	110	65	36.26
15	70	1.5	90	81	38.16
16	70	2.0	70	83	38.38

In this design method, the largest S/N ratio denoted the best level. Fig. 8 shows that there was a different dependence between control factors and the S/N ratio with experimental data. Compared with the stirring speed, the yield showed greater dependence on the amount of sulfuric acid and temperature. The stirring speed had little effect on the product yield, and there was a highly similar and large effect on the yield of ring-opening polymerization between temperature and sulfuric acid. However, a very clear comparison for each influencing factor on the yield could not be reflected perfectly. A comparison of the degree of influence of each factor can be

Table 2 Parameters and levels for hydrosilylation

Influencing factor	Level 1	Level 2	Level 3	Level 4
D: temperature (°C)	70	80	90	100
E: chloroplatinic acid amount (wt%)	0.002	0.003	0.004	0.005
F: stirring speed (rpm)	150	170	190	210

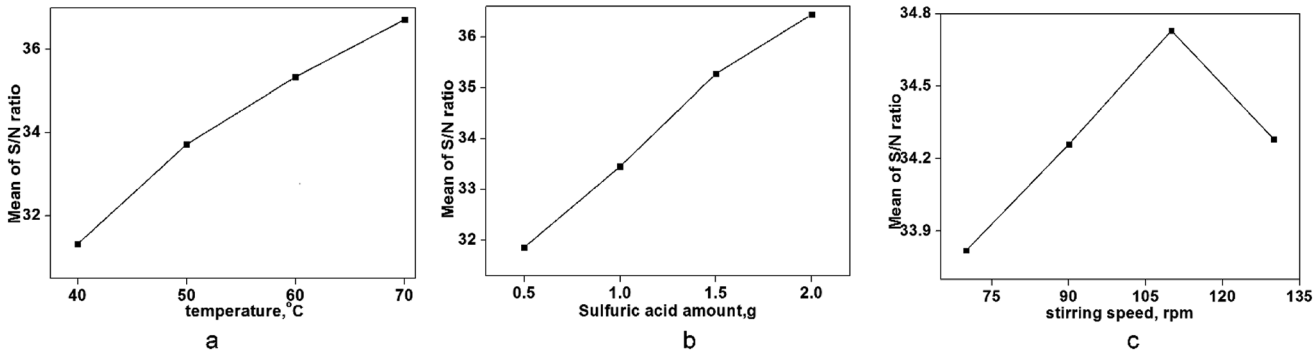

Fig. 8 Trend of factors on the S/N ratio (ring-opening polymerization).

Table 4 Experimental design of hydrosilylation

Strain	A, °C	B, wt%	C, rpm	Yield, %	S/N
1	70	0.002	150	46	33.26
2	70	0.003	170	56	34.96
3	70	0.004	190	59	35.41
4	70	0.005	210	67	36.52
5	80	0.002	170	54	34.65
6	80	0.003	150	68	36.65
7	80	0.004	210	73	37.27
8	80	0.005	190	72	37.15
9	90	0.002	190	60	35.56
10	90	0.003	210	78	37.84
11	90	0.004	150	80	38.06
12	90	0.005	170	82	38.28
13	100	0.002	210	64	36.12
14	100	0.003	190	85	38.59
15	100	0.004	170	80	38.06
16	100	0.005	150	81	38.17

reflected by the contribution ratio, and the dependence of each factor on the yield of this ring-opening polymerization could be presented in detail.

Correlation calculations of ANOVA were done to evaluate the results of the experimental design. As shown in Table 5, the dependence of the above factors had a significant effect on the yield. According to the contribution ratio, an order of A > B > C could be determined. Temperature was the biggest factor that could affect the yield, with contribution ratio of 55.44%. By contrast, the contribution ratio of 0.97% of stirring speed displayed the smallest effect on the yield.

In general, a higher S/N ratio denotes an optimal level of the influencing factor.[24,25] According to the contribution ratio and data in Fig. 8, the order of A4B4C3 (*i.e.*, temperature of 70 °C, sulfuric acid of 2.0 g, and a stirring speed of 110 rpm, respectively) was seen as the optimal combination of factors with respect to the yield. A yield of 87.2% was shown in a realistic experiment using this optimal combination. A higher yield was shown by increasing the temperature due to more intermolecular collisions at a higher temperature, and the same reason explained the effect of sulfuric acid on the yield.[26] As the catalyst amount increases, more D4 molecules can interact with catalyst molecules.[27,28] However, a distinct trend was shown in Fig. 8c; the main reason was that a low stirring speed (<110 rpm) could provide sufficient time to generate interactions between D4 and the catalyst.

Table 5 Analysis of variance of factors on the yield of ring-opening polymerization

Project	Sum of square, SS	Degree of freedom, *f*	Mean square, MS	*F* value	Contribution ratio, %
A	64.56	3	21.52	119.55	55.44
B	48.76	3	16.25	90.28	41.74
C	1.64	3	0.55	3.06	0.97
Error	0.53	3	0.18		2.26

Table 6 Analysis of variance of factors on the yield of hydrosilylation

Project	Sum of square, SS	Degree of freedom, *f*	Mean square, MS	*F* value	Contribution ratio, %
D	17.6	3	5.87	83.56	49.22
E	17.07	3	5.69	81.29	47.72
F	0.48	3	0.16	2.29	0.8
Error	0.2	3	0.07		2.97

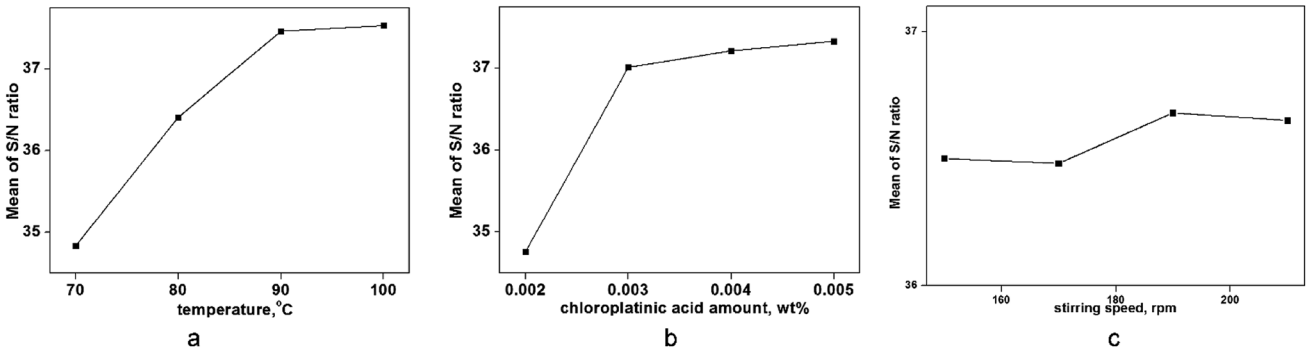

Fig. 9 Trend of factors on the S/N ratio (hydrosilylation).

Table 7 Phase behavior of siloxane in toluene at 25 °C (λ_{max} = 206 nm)

Solvent	Content (siloxane), wt%	25 °C, A	35 °C, A	45 °C, A	55 °C, A
Toluene	0	0.312	0.306	0.310	0.314
Toluene	1	0.306	0.310	0.308	0.311
Toluene	2	0.311	0.305	0.312	0.307
Toluene	3	0.312	0.307	0.310	0.313

3.4 Taguchi design for hydrosilylation

To evaluate the best combination for a maximum yield of hydrosilylation, an experiment using the Taguchi design (shown in Table 4) and the range of each factor was selected according to single-factor analyses. The ANOVA calculation was conducted using the S/N ratios given in Table 6, and the combination of these factors that were significant for the yield obtained. According to the contribution ratios given in Table 6, the experimental factors that had a major impact were (in descending order) were temperature (D), amount of chloroplatinic acid (E) and stirring speed (F). As seen in Fig. 9 and Table 4, the optimum combination for the maximum yield in hydrosilylation was D4E2F3 (temperature of 100 °C, amount of chloroplatinic acid of 0.003 wt%, and a stirring speed of 190 rpm). A yield of 84.7% was observed in an actual experiment at this combination.

3.5 Phase behavior of siloxane in organic liquids and phase behavior of toluene, thickener and CO_2

Silicone cannot be dissolved separately at high-pressure CO_2, which has been shown by a high-pressure dissolution experiment.[11,29–31] According to the literature[10,31] and a high boiling point (110.6 °C), toluene is an excellent organic liquid to thicken CO_2. Compared with hexane, a smaller amount is another important reason to choose toluene.[32] Other solvents were excluded due to the large amount needed and poor thickening performance.[9,33,34]

To evaluate the solubility of the thickener in toluene, a mixed solution containing siloxane was placed in a glass bottle and stirred evenly at 25 °C. Then, the mixed solution was transferred to a cuvette to measure the absorbance by a UV-visible spectrophotometer at an absorption peak of 206 nm (toluene). In general, absorbance was almost constant with increasing polymer amount in toluene if the polymer and toluene could dissolve each other. By contrast, a turbid solution or gel would demonstrate poor solubility.

As seen in Table 7, these solutions containing different amounts of polymer (1 wt% to 3 wt%) were compared with pure toluene, but there was no difference visually between the solutions and pure toluene, and all solutions exhibited a single phase. Moreover, the stable absorbance illustrated excellent solubility of the thickener in toluene. As shown in Table 8, the viscosity of toluene increased with increasing polymer content at room pressure. Thus, this polymer could be used as a thickener of toluene, and the prepared polymer was soluble in toluene.

Moreover, the solubility of the prepared polymer in CO_2 was measured from 20 °C to 50 °C and pressures of 6 MPa to 14 MPa. A single-phase state was observed visually (this was the only basis for determining dissolution) and phase behavior was observed mainly through the glass window of the dissolution equipment. Fig. 10 illustrates different phase behaviors, and single-phase status (dissolution) is shown in Fig. 10(3). Results showed that all cloud points at different temperatures and concentrations were <8 MPa.

Table 8 Viscosity (mPa s) of toluene solution containing prepared siloxane at room pressure

Solvent	Content (siloxane), wt%	25 °C	35 °C	45 °C	55 °C
Toluene	0	0.582	0.576	0.568	0.563
Toluene	1	0.586	0.575	0.570	0.566
Toluene	2	0.583	0.579	0.575	0.568
Toluene	3	0.601	0.592	0.585	0.578

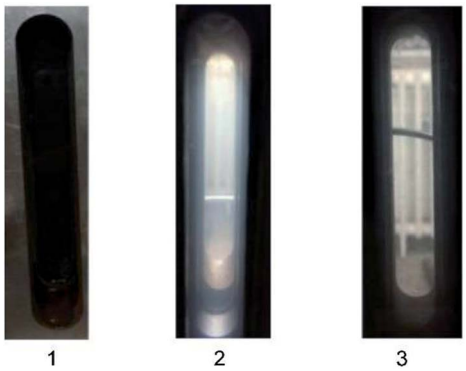

Fig. 10 Phase behavior of liquid CO_2 containing the siloxane and 3-fold toluene (wt%). (1) Deep turbid state. (2) Mild turbid state. (3) Clarified state.

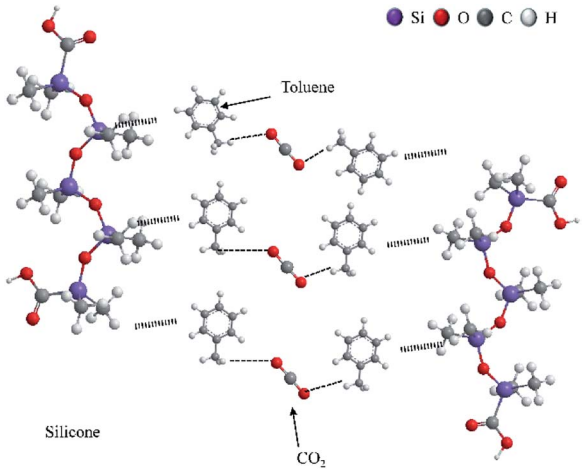

Fig. 12 Thickening mechanism of silicone polymer in liquid CO_2.

3.6 Thickening property of siloxane in CO_2

As shown in Fig. 11a, the viscosity of thickened liquid CO_2 decreased with increasing flow rate at 0.1–0.7 mL min^{-1}. The thickened liquid CO_2 was considered to be a non-Newtonian fluid, which had shear thinning,[29,35] and the mesh structures formed among these three chemicals were destroyed by the shearing action with increasing flow rate.[36] Fig. 11b shows a clear and significant reduction in CO_2 viscosity between 295 K and 335 K that was attributable to the effect of temperature on rheology. The change in CO_2 viscosity was based mainly on changes in some of the properties of these mesh structures: spreading area of each mesh structure, density among grid structures, bond strength, and interaction forces among molecules (silicone polymer, toluene and CO_2).[37,38] The microscopic migration rate and activity of various molecules increased obviously with rising temperature, which resulted in fractures of bonds among molecules and damage to the grid structure formed by molecules. More specifically, the activation energy of molecules decreased from 295 K to 335 K, which resulted in reduced viscosity.[29] A rising trend on viscosity was shown from 8 MPa to 14 MPa because the increased pressure could significantly reduce cracking of the mesh structure and molecular spacing.[30]

To compare the thickening performance of epoxy-terminated polydimethylsiloxane in CO_2, a commercial polydimethylsiloxane with the same M_n (21 000) was used to evaluate CO_2 viscosity. PDMS displayed a weaker thickening performance than that of the modified siloxane at the same measurement conditions. Studies[39,40] have shown that polydimethylsiloxane has a poor thickening property in liquid CO_2. Doherty[32] prepared a silicone thickener that could increase CO_2 viscosity significantly (300-fold), but the poor solubility, high dissolution pressure and co-solvent content hindered application of silicone for thickening CO_2.

3.7 Thickening mechanism of prepared silicone in CO_2

In previous studies, the thickening mechanism focused mainly on fluoropolymers and hydrocarbon polymers.[6–8,41] By contrast, the thickening mechanism of siloxane in CO_2 has not been proposed before. The thickening mechanism of silicone is similar to that of a surfactant,[29] but the addition of a solvent is the biggest difference between two thickeners.[29,42]

As an electron-donating group, the phenyl group in toluene could interact with CO_2 (ref. 43) to generate an induction force.

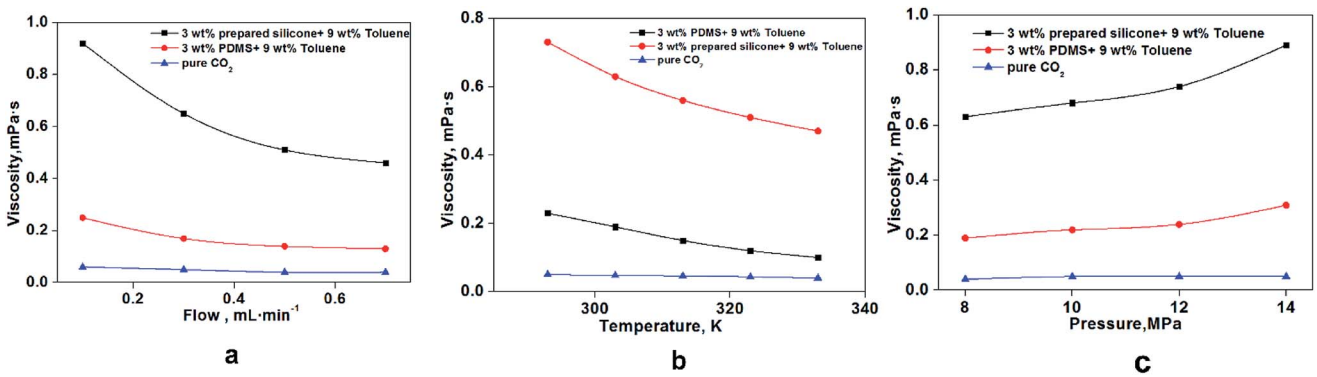

Fig. 11 Effect of different factors on the viscosity of thickened CO_2. (a) Effect of flow rate at 8 MPa and 303 K; (b) temperature effect at 8 MPa and 0.3 mL min^{-1}; (c) pressure effect at 303 K and 0.3 mL min^{-1}.

Moreover, the C–H–O bond is the other reason to promote interaction between CO_2 and toluene.[44–47]

The interaction between silicone and toluene was considered to be a non-polar bond according to the similar polarity between silicone and toluene.[48,49] Several mesh structures were formed among toluene, CO_2 and siloxane using the interactions mentioned above, and Li and colleagues proposed a theory of the thickening mechanism similar to that for silicone.[1] Numerous mesh structures showed an increase in liquid viscosity macroscopically.[29] The epoxy group and carbonyl group within the ester group could assist this prepared polymer to enhance the interaction between the polymer and CO_2, and solubility and miscibility could be improved.[6,50,51]

4. Conclusions

To obtain an excellent yield, the prepared process of epoxy-terminated polydimethylsiloxane was optimized by a Taguchi method. This method could lead to obtaining optimal prepared parameters with considerably fewer experiments. Compared with polydimethylsiloxane, the thickened CO_2 added to the modified siloxane showed a highly thickening performance for CO_2 viscosity, and the thickened CO_2 showed shear thinning. Increasing pressure was beneficial for improving CO_2 viscosity. However, a decreasing trend was shown with increasing temperature. The prepared siloxane presented an excellent thickening performance and high recyclability for CO_2 viscosity. Experimental results showed that this modified siloxane could be used to thicken CO_2 (Fig. 12).

Conflicts of interest

There are no conflicts to declare.

Acknowledgements

We send special gratitude to the Shandong Province Foam Fluid Efficient Exploitation of Oil and Gas Engineering Research Centre in the China University of Petroleum (East China). We thank Binfei Li for helping in the design of the capillary viscometer.

References

1 Q. Li, Y. Wang, Q. Li, G. Foster and C. Lei, *RSC Adv.*, 2018, **8**, 8770–8778.
2 S. Ayatollahi, A. Hemmati-Sarapardeh, M. Roham and S. Hajirezaie, *J. Taiwan Inst. Chem. Eng.*, 2016, **63**, 107–115.
3 F. Zhao, H. Hao, J. Hou, L. Hou and Z. Song, *J. Pet. Sci. Eng.*, 2015, **133**, 52–65.
4 H. Kang, H. Lv, F. Gao, X. Meng and Y. Feng, *Int. J. Coal Geol.*, 2018, **196**, 19–28.
5 S. Zhang, Y. She and Y. Gu, *J. Chem. Eng. Data*, 2011, **56**, 1069–1079.
6 Y. Wang, L. Hong, D. Tapriyal, I. C. Kim, I. Paik, J. M. Crosthwaite, A. D. Hamilton, M. C. Thies, E. J. Beckenman, R. M Enick and J. K. Johnson, *J. Phys. Chem. B*, 2009, **113**, 14971–14980.
7 A. Dardin, J. M. DeSimone and E. T. Samulski, *J. Phys. Chem. B*, 1998, **102**, 1775–1780.
8 C. F. Kirby and M. A. McHugh, *Chem. Rev.*, 1999, **99**(2), 565–602.
9 L. L. Williams, J. B. Rubin and H. W. Edwards, *Ind. Eng. Chem. Res.*, 2004, **43**, 4967–4972.
10 J. H. Bae and C. A. Irani, *SPE Advanced Technology Series*, 1993, **1**, 166–171.
11 M. J. O'Brien, R. J. Perry, M. J. Doherty, J. J. Lee, A. Dhuwe, E. J. Beckman and R. M. Enick, *Energy Fuels*, 2016, **30**, 5990–5998.
12 Z. B. Gonder, S. Arayici and H. Barlas, *Sep. Purif. Technol.*, 2011, **76**, 292–302.
13 D. Yu, C. Wang, X. Cheng and F. Zhang, *Appl. Surf. Sci.*, 2008, **255**, 1865–1869.
14 G. Taguchi and Y. Yokoyama, *Taguchi methods: design of experiments*, American Supplier Institute (ASI) Press, Tokyo, Japan, 1993.
15 Y. C. Chen, P. J. Tsai and J. L. Mou, *Environ. Sci. Technol.*, 2008, **42**, 5298–5303.
16 C. Ramírez, M. Rico, A. Torres, L. Barral, J. López and B. Montero, *Eur. Polym. J.*, 2008, **44**, 3035–3045.
17 S. S. Hou, Y. P. Chung, C. K. Chan and P. L. Kuo, *Polymer*, 2000, **41**, 3263–3272.
18 M. Y. Chang, G. J. Tsai and J. Y. Houng, *Enzyme Microb. Technol.*, 2006, **38**, 407–414.
19 J. L. Rosa, A. Robin, M. B. Silva, C. A. Baldan and M. P. Peres, *J. Mater. Process. Technol.*, 2009, **209**, 1181–1188.
20 R. K. Roy, *Design of Experiments Using the Taguchi Approach: 16 Steps to Product and Process Improvement*, Wiley, New York, 2001.
21 S. Ranganathan, J. Tebbe, L. O. Wiemann and V. Sieber, *Process Biochem.*, 2016, **51**, 1479–1485.
22 A. C. Aycaguer, M. Lev-On and A. M. Winer, *Energy Fuels*, 2001, **15**, 303–308.
23 H. J. C. De. Souza, C. B. Moyses, F. J. Pontes, R. N. Duarte, C. E. S. Silva, F. L. Alberto, U. R. Ferreira and M. B. Silva, *Mol. Cell. Probes*, 2011, **25**, 231–237.
24 R. Chauhan, T. Singh, N. Kumar, A. Patnaik and N. S. Thakur, *Appl. Therm. Eng.*, 2017, **116**, 100–109.
25 A. Mehta, R. Siddique, B. P. Singh, S. Aggoun, G. Łagód and D. B. Hunek, *Constr. Build. Mater.*, 2017, **150**, 817–824.
26 F. Bernard, D. K. Papanastasiou, V. C. Papadimitriou and J. B. Burkholder, *J. Phys. Chem. A*, 2018, **122**, 4252–4264.
27 D. W. Scott, *J. Am. Chem. Soc.*, 1946, **68**, 356–358.
28 T. C. Kendrick, B. Parbhoo and J. W. White, *Organic Silicon Compounds*, 1989, vol. 1, pp. 1289–1361, DOI: 10.1002/0470025107.ch21.
29 X. Luo, S. Wang, Z. Wang, Z. Jing, M. Lv, Z. Zhai and T. Han, *J. Pet. Sci. Eng.*, 2015, **133**, 410–420.
30 R. M. Enick and J. Ammer, *A literature review of attempts to increase the viscosity of dense carbon dioxide*, Website of the National Energy Technology Laboratory, 1998, http://citeseerx.ist.psu.edu/viewdoc/download?doi=10.1.1.167.1728&rep=rep1&type=pdf.

31 J. H. Bae, *SPE International Symposium on Oilfield Chemistry*, 1995, pp. 47–54, DOI: 10.2118/28950-MS.
32 M. D. Doherty, J. J. Lee, A. Dhuwe, M. J. O'Brien, R. J. Perry, E. J. Beckman and R. M. Enick, *Energy Fuels*, 2016, **30**, 5601–5610.
33 J. P. Heller, D. K. Dandge, R. J. Card and L. G. Donaruma, *SPE J.*, 1985, **25**, 679–686.
34 F. M. Llave, F. T. H. Chung and T. E. Burchfield, *SPE Reservoir Eng.*, 1990, **5**, 47–51.
35 S. Mortazavi, *Chin. J. Chem. Eng.*, 2017, **25**, 1360–1368.
36 X. Sun, X. Liang, S. Wang and Y. Lu, *J. Pet. Sci. Eng.*, 2014, **119**, 104–111.
37 P. C. Harris and P. M. Pippin, *SPE Prod. Facil.*, 2000, **15**, 27–32.
38 H. Bahrami, R. Rezaee, D. Nazhat and J. Ostojic, *APPEA J.*, 2011, **51**, 639–652.
39 S. Cai, MPhil, Texas A&M University, 2010, https://oaktrust.library.tamu.edu/handle/1969.1/ETD-TAMU-2010-08-8375.
40 Z. Al. Yousef, MPhil, Texas A&M University, 2012, https://oaktrust.library.tamu.edu/handle/1969.1/ETD-TAMU-2012-08-11698.
41 G. G. Yee, J. L. Fulton and R. D. Smith, *J. Phys. Chem.*, 1992, **96**, 6172–6181.
42 S. Cummings, D. Xing, R. Enick, S. Rogers, R. Heenan, I. Grillo and J. Easto, *Soft Matter*, 2012, **8**, 7044–7055.
43 T. Sarbu, T. J. Styranec and E. J. Beckman, *Ind. Eng. Chem. Res.*, 2000, **39**, 4678–4683.
44 P. Raveendran and S. L. Wallen, *J. Am. Chem. Soc.*, 2002, **124**, 12590–12599.
45 M. A. Blatchford, P. Raveendran and S. L. Wallen, *J. Am. Chem. Soc.*, 2002, **124**, 14818–14819.
46 T. Tsukahara, Y. Kayaki, T. Ikariya and Y. Ikeda, *Angew. Chem., Int. Ed.*, 2004, **43**, 3719–3722.
47 B. Chandrika, L. K. Schnackenberg and P. S. L. Wallen, *Chem.–Eur. J.*, 2005, **11**(21), 6266–6271.
48 I. Montes, C. Lai and D. Sanabria, *J. Chem. Educ.*, 2003, **80**, 447.
49 J. Wang, J. H. Horton, G. Liu, S. Y. Lee and K. J. Shea, *Polymer*, 2007, **48**, 4123–4129.
50 S. Kilic, S. Michalik, Y. Wang, J. K. Johnson, R. M. Enick and E. J. Beckman, *Ind. Eng. Chem. Res.*, 2003, **42**, 6415–6424.
51 M. A. Blatchford, P. Raveendran and S. L. Wallen, *J. Phys. Chem. A*, 2003, **107**, 10311–10323.